JAASP http://www.aaspjournal.org
Journal of Asian Association of Schools of Pharmacy 2024; 13: 1–5
doi: https://doi.org/10.62100/jaasp.2023-06

Research Paper

Weak electric current increases ceramide levels by inducing ceramide synthase expression

Naoshi Yamazaki[1], Chiho Ohtsuka[2] and Kentaro Kogure[1,3,*]

[1]*Graduate School of Biomedical Sciences, Tokushima University, Tokushima, Japan*
[2]*Faculty of Pharmaceutical Sciences, Tokushima University, Tokushima, Japan*
[3]*Innovative Research Center for Drug Delivery System, Graduate School of Biomedical Sciences, Tokushima University, Tokushima, Japan*

Received December 7, 2023
Revised January 18, 2024
Revised January 25, 2024
Accepted January 26, 2024

* Corresponding author
Graduate School of Biomedical Sciences,
Tokushima University, Shomachi 1-78,
Tokushima 770-8505, Japan
E-mail: kogure@tokushima-u.ac.jp

ABSTRACT

We previously demonstrated that weak electric current (WEC) induces the skin penetration of macromolecules by the cleavage of intercellular junctions and allows for incorporation of macromolecules into cells via endocytosis. We further showed that WEC facilitates the leakage of macromolecules from endosomes to cytoplasm and that this phenomenon correlates with increased endosomal ceramide levels. From these observations, it suggested ceramide production is induced by WEC. In this study, to investigate mechanisms by which WEC treatment increases ceramide levels, acyl chains in ceramides of WEC-treated cells were analyzed. As a result, we found that WEC increased the amounts of C16:0, C22:0, and C24:1 ceramides and that WEC induced ceramide synthase 2 expression. Therefore, we conclude that WEC activates the ceramide synthesis pathway and that increased endosomal ceramide would contribute to the leakage of macromolecules.

Key words: weak electric current, ceramide synthesis, cytoplasmic delivery

1. Introduction

Permeation of ionized molecules into the skin can be induced by weak electric current (WEC; 0.3~0.5 mA/cm^2) (Kalia et al., 2004; Karpiński 2018). This technology, called iontophoresis, is utilized for intradermal drug delivery. We previously demonstrated that various nucleic acids and liposomes were successfully delivered into rat and mouse skins by WEC treatment (Kigasawa et al., 2010, 2011; Kajimoto et al., 2011). We also demonstrated that when rat skin and culture cells were treated with WEC, the expression level of connexin 43 was decreased, and the depolymerization of actin was promoted (Hama et al., 2014). Because connexin 43 is a gap-junction protein and polymerized actin associates with tight-junction structures, these observations suggested that skin penetration of hydrophilic macromolecules by WEC is facilitated by the cleavage of intercellular junctions.

Further analyses demonstrated that siRNA delivered into mouse skin resulted in decreased expression of target mRNA (Kigasawa et al., 2010). Because siRNA mediates degradation of mRNA via interactions that occur in the cytoplasmic space, this result suggests that WEC-delivered siRNA reaches the cytoplasm; we also demonstrated by using culture cells that the WEC-induced cellular uptake of siRNA is mediated by endocytosis (Hasan et al., 2016a). Notably, unmodified siRNA molecules are known to not escape efficiently from conventional endosomes, such as clathrin-coated endosomes and macropinosomes. Therefore, in WEC-treated cells, cytoplasmic delivery of siRNA via endosomes is likely to occur by non-conventional endocytic mechanisms. Intriguingly, we found that lower molecular weight fluorescein isothiocyanate (FITC)-dextran molecules (< 10 kDa) became widely dispersed in the cytoplasm of culture cells after treatment with WEC, whereas higher molecular weight FITC-dextran (> 70 kDa) remained in the endosomes (Hasan et al., 2016b). This observation showed that WEC-induced endosomes have unique structural properties that allow for leakage of smaller macromolecules having molecular mass of less than 70 kDa.

Recently, we showed that WEC-induced endosomes exhibit an elliptical shape, and that these endosomes are enriched in ceramides (Torao et al., 2020). In addition, the amount of total cellular ceramide in WEC-treated cultured mouse cells was shown to be 1.8-fold higher than that of untreated cells, and that of WEC-treated mouse skin was 1.86-fold higher than that of untreated skin (Torao et al., 2020). These results suggest that WEC treatment induces

ceramide synthesis and that ceramides are important to the mechanism of cytoplasmic delivery.

Ceramide has been shown to induce membrane permeabilization in the mitochondrial outer membrane (Siskind et al., 2002). To explain this phenomenon, two mechanisms have been proposed. One mechanism is that ceramides form a pore structure, called a "ceramide channel," in the mitochondrial outer membrane; this channel may permit the release of proteins with molecular mass less than 60 kDa from the intermembrane space of mitochondria (Perera et al., 2016). A second, ceramide channel-independent mechanism of ceramide-induced membrane permeabilization involves the surface mismatch between the two monolayers of the lipid bilayer (Artetxe et al., 2017). Based on these hypotheses, we suggest that the increase of the ceramide content of endosomal membranes under WEC could induce the leaking of macromolecules from endosomes to the cytoplasm.

In this study, we analyzed the mechanism by which WEC treatment increases the amount of cellular ceramide. We first characterized the specific ceramide molecules that are induced in WEC-treated culture cells by liquid chromatography-tandem mass spectrometry (LC-MS/MS). In addition, the effect of selective ceramide synthesis pathway inhibitor on ceramide synthesis by WEC-treated cells was examined. These chemical and pharmacological results were correlated with the effect of WEC treatment on the level of expression of ceramide synthases in the *de novo* ceramide synthesis pathway.

2. Materials and methods

2.1. Materials

All reagents used in this study were commercially available and used without further modification, and experimental procedures were performed essentially as recommended by the manufacturer.

2.2. WEC treatment of cultured cells

The mouse melanoma cell line B16-F1 (Dainippon Sumitomo Pharma Biomedical, Osaka, Japan) was cultured at a density of 2.5×10^4 to 2.0×10^5 cells per 35-mm dish in Dulbecco's modified Eagle medium (DMEM) containing 4.5 g/L glucose (Nacalai Tesque, Kyoto, Japan) supplemented with 10% fetal bovine serum (FBS) (BioWest, Nuaillé, France) at 37°C in a 5% CO_2 atmosphere. After 24 hr, cells were washed with Dulbecco's phosphate-buffered saline (D-PBS) without calcium and magnesium, then one milliliter of DMEM without FBS (DMEM-FBS) was added to the dish. WEC treatment was performed by placing Ag-AgCl electrodes (3M, Saint Paul, MN, USA) into the dish and treating the cells with a constant WEC of 0.34 mA/cm^2 for 15 min. According to the conditions reported by us (Torao et al., 2020), applied current and application time were set.

2.3. Lipid extraction

B16-F1 cells (2.0×10^5 cells/35-mm dish) were treated with WEC and then incubated for 24 hr at 37°C. The culture dishes were washed with D-PBS, and the cells were collected in 800 μL of 2% potassium chloride. The cells were lysed by sonication, and the protein concentration was measured with the BCA protein assay kit (Thermo Fisher Scientific, Waltham, MA, USA) using bovine serum albumin (BSA) as a standard. Total lipids were then extracted from 720 μL of the sonicated sample with the Bligh and Dyer method (Bligh and Dyer, 1959). Briefly, 2 mL of methanol, 2 mL of chloroform, and 10 μL (50 pmols) of C12:0 ceramide (Cayman Chemical, Ann Arbor, MI, USA) as an internal control were added to the sonicated sample. After addition of 1 mL water, the samples were mixed well and centrifuged at 1100*g* for 5 min at 4°C. After separation of the water-soluble and -insoluble phases, the insoluble phase was carefully collected. To the soluble phase, 1 mL of methanol/chloroform (3:17, v/v) was added, and the sample was mixed well. After centrifugation, the insoluble phase was carefully collected and combined with the first insoluble phase. The insoluble phase containing the extracted lipids was dried under nitrogen gas.

2.4. Analysis of cellular lipids

The extracted lipids were dissolved in 100 μL of methanol/formic acid (99:1, v/v) containing 5 mM ammonium formate. For liquid chromatographic separation, methanol/formic acid (99:1, v/v) containing 5 mM ammonium formate was used as the mobile phase with an isocratic flow of 300 μL/min. LC-MS/MS analyses were performed with a 4000 QTRAP LC-MS/MS System (SCIEX, Framingham, MA, USA) using a Cadenza CD-C18 column (IMTAKT, Kyoto, Japan). The multiple reaction monitoring transitions measured were m/z $[M+H]^+$ to m/z 264, which represent the fragment ion of sphingosine. After LC-MS/MS analyses, the amounts of ceramide molecules were calculated by comparison with signal from the internal control (C12:0 ceramide); the correction factor 0.995 was used for ceramides C14:0 to C20:0 and 1.472 was used for ceramides containing an *N*-acyl group longer than C22. The ceramide levels in multiple samples were normalized to total protein.

2.5. Inhibition of ceramide synthesis pathway and immunostaining of cellular ceramide

Fumonisin B1 (Cayman Chemical) was dissolved in dimethyl sulfoxide and diluted in DMEM-FBS. B16-F1 cells (2.5 or 5.0×10^4 cells/35-mm dish) were cultured for 24 hr then washed with D-PBS. Cells were treated with vehicle or fumonisin B1 (25 μM) for 1 hr, then treated with WEC as described in Section 2.2. After incubation for 24 hr, cells were washed with D-PBS and treated with 4% paraformaldehyde for 20 min at 37°C. After three washes with D-PBS containing 1% BSA (PBS-B), the cells were

permeabilized by incubation for 20 min at 37°C in PBS-B containing 0.1% Triton X-100 and then washed with PBS-B. An anti-ceramide antibody (diluted 1:100 in PBS-B; Merck, Darmstadt, Germany) was added to the dish, and the samples were incubated for 1 hr at 37°C. Following three washes, an Alexa Fluor 488-labeled secondary antibody (diluted 1:500 in PBS-B; Abcam, Cambridge, UK) was added, and the cells were incubated for 1 hr at 37°C. The nuclei were counterstained by incubation with DAPI (1 μg/mL in D-PBS; Dojindo, Kumamoto, Japan) for 15 min at 37°C. After a final wash, the cells were observed with confocal laser scanning microscopy (LSM700, Carl Zeiss, Oberkochen, Germany). The relative fluorescence was quantified using Image J software (National Institutes of Health, MD, USA). At one experiment, we obtained immunostaining intensity data from each eight areas of control cells (not subjected to WEC and not treated with inhibitor), WEC-treated cells without inhibitor, and WEC-treated cells with inhibitor. The average of intensity obtained from eight areas of control cells was set as 1.0, the intensity of each area was relatively calculated. The data of 48 areas obtained from six independent experiments were used for depiction of graph and for statistically analysis.

2.6. Quantitative mRNA analysis

Expression levels of ceramide synthase isoforms were analyzed by reverse transcription-quantitative polymerase chain reaction (RT-qPCR). B16-F1 cells (2.0×10^5 cells/35-mm dish) were treated with WEC as described in Section 2.2. After 1, 6, or 24 hr of incubation following WEC treatment, cellular RNA was isolated with the NucleoSpin RNA kit (MACHEREY-NAGEL, Düren, Germany). Two hundred ng of total RNA was reverse transcribed using PrimeScript RT Master Mix, which included an oligo(dT) primer and random hexamers (TaKaRa Bio, Ohtsu, Japan). Mixtures (10 μL) were incubated at 37°C for 15 min, then at 85°C for 5 sec. Samples (2 μL) of the reverse transcribed mixtures were amplified with specific primer pairs (0.4 μM) for ceramide synthases (Becker et al., 2008) and glyceraldehyde 3-phosphate dehydrogenase (Leong et al., 2010) using TB Green Premix Ex Taq II (TaKaRa Bio). The PCR cycle involved an initial melt at 95°C for 30 sec, then 40 cycles of 95°C for 5 sec and 60°C for 30 sec, and was performed in a Thermal Cycler Dice Real Time System III (TaKaRa Bio). Ct values were obtained with the second derivative maximum method, and the relative mRNA levels were evaluated with the ΔΔCt method using glyceraldehyde 3-phosphate dehydrogenase as an internal control.

2.7. Statistical analysis

The results were expressed as the mean ± standard deviation (SD). Statistical analyses were performed using Welch's *t* test. P-values < 0.05 were considered statistically significant and are indicated by an asterisk (*).

3. Results and Discussion

3.1. Identification of specific ceramides induced by WEC treatment

Previously, we showed that the total amount of ceramide is increased in mammalian cells and in skin tissue by WEC treatment (Torao et al., 2020). In the present study, we further characterized this increase by investigating the specific *N*-acyl groups of the ceramides produced upon subjection to WEC. Specifically, we performed LC-MS/MS analyses of lipids extracted from WEC-treated mouse B16-F1 cells, and the amount of each type of ceramide was quantified. According to this analysis, ceramide molecules containing C16:0, C22:0, and C24:1 *N*-acyl groups were significantly increased when cells were treated with WEC (Fig. 1). This observation suggests that WEC treatment induces pathways leading to the synthesis of C16:0, C22:0, and C24:1 ceramides.

3.2. Identification of steps in the ceramide synthesis pathway induced by WEC

Three ceramide synthesis pathways are currently known to exist in mammals: the sphingomyelinase pathway, in which sphingomyelin is degraded by neutral sphingomyelinase; the salvage pathway, in which sphingomyelin is degraded by acid sphingomyelinase; and the *de novo* synthesis pathway (Taniguchi and Okazaki, 2021). Previously, we reported that the addition of inhibitors of neutral sphingomyelinase and acid sphingomyelinase did not change the amount of ceramide in WEC-treated cells (Torao et al., 2020). This result suggested that WEC treatment increases ceramide production via the *de novo* synthesis pathway.

Therefore, in this study, we examined the effect of WEC on the *de novo* synthesis pathway. This pathway consists of

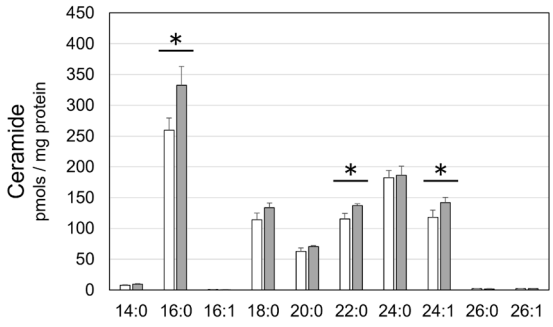

Figure 1. Amount of ceramide molecules in WEC-treated and untreated cells.

B16-F1 cells were mock-treated or treated with WEC (n = 3) and then incubated for 24 hr. Cellular lipids were extracted from the cells, and ceramide molecules were identified by LC-MS/MS. The level of each ceramide was calculated by comparison to the internal control C12:0 ceramide, and ceramide levels were normalized to total cellular protein. White and gray columns show WEC-untreated and treated cells, respectively. Data are displayed as mean ± SD (n = 3). *P < 0.05.

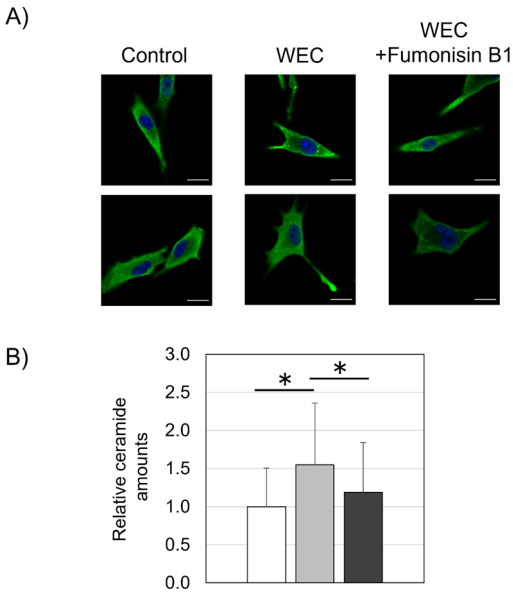

Figure 2. Effect of ceramide synthase inhibition on cellular ceramide levels.
Cells were incubated with vehicle or fumonisin B1 and then treated with WEC. Ceramides were quantified using immunofluorescence with an anti-ceramide antibody. (A) Typical images from the immunostaining. Ceramides and nuclei are represented by green and blue signals, respectively. Control cells were not treated with inhibitor and were not subjected to WEC. (B) The fluorescence intensities are relative to the signal from cells not treated with inhibitor and not subjected to WEC (control cells), which were assigned an intensity value of 1.0. White, gray, and black columns show control cells, WEC-treated cells without inhibitor, and WEC-treated cells with inhibitor, respectively. Data are mean ± SD (n = 48). *P < 0.05.

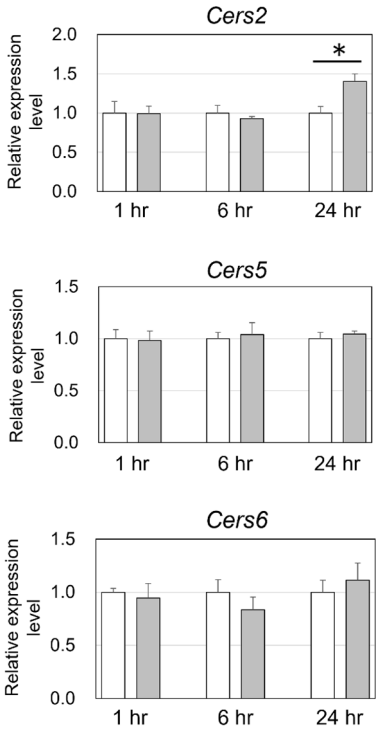

Figure 3. Effect of WEC treatment on the expression of ceramide synthase isoforms.
B16-F1 cells were mock-treated or treated with WEC (n = 3), then incubated (for 1, 6, or 24 hr) and total RNA was isolated and reverse transcribed. The cDNA was amplified by qPCR using the specific primer pairs. Each qPCR assay was performed in duplicate or triplicate, and the average of the Ct values was used for analysis. The mRNA level of each ceramide synthase is shown relative to the value obtained from cells not subjected to WEC but incubated for the same time. White and gray columns show data from untreated and WEC-treated cells, respectively. Data are mean ± SD (n = 3). *P < 0.05.

multiple steps, each catalyzed by dedicated enzymes. In the first step of this pathway, serine *C*-palmitoyltransferase synthesizes 3-dehydrosphinganine from serine and palmitoyl-CoA. In the second step, 3-dehydrosphinganine is reduced to dihydrosphingosine by 3-dehydrosphinganine reductase. Then, dihydrosphingosine *N*-acyl transferase, also known as ceramide synthase, transfers the acyl group of specific acyl-CoA molecule to dihydrosphingosine to form *N*-acyl dihydrosphingosine (also called dihydroceramide). Finally, ceramide is produced by dihydroceramide desaturase.

WEC treatment increased the amount of C16:0, C22:0, and C24:1 ceramides (Fig. 1) and mammalian cells possess several ceramide synthases which utilize specific acyl groups as substrates (Levy and Futerman, 2010). From these observations, we predicted that ceramide synthases which produce C16:0, C22:0, and C24:1 dihydroceramides were induced by WEC. Therefore, we used fumonisin B1, an inhibitor of ceramide synthases (Hoeferlin et al., 2013) to analyze the relationship of this step in ceramide synthesis pathway to the impact of WEC treatment. According to preliminary analyses of the inhibitory activity and cell toxicity of inhibitor, we treated cells with 25 μM fumonisin B1 for 1 hr prior to WEC treatment. Under these conditions, treatment with fumonisin B1 decreased the amount of cellular ceramide in WEC-treated cells (Figs. 2A and B). This result suggested that ceramide synthases represent the key component linking the *de novo* synthesis pathway to the increase of cellular ceramide production by WEC treatment.

3.3. WEC treatment selectively induces the expression of ceramide synthase isoforms

The selective nature of the ceramide increase (Fig. 1) led us to investigate the role of specific ceramide synthases in the impact of WEC treatment on cellular ceramide levels. In human and mouse, the diversity of ceramide acyl chains is due to the presence of 6 isoforms of ceramide synthase, each with a characteristic specificity for acyl groups (Becker et al., 2008). In particular, ceramide synthase 5 (encoded by *Cers5*) and ceramide synthase 6 (*Cers6*) favor the transfer of C16 acyl groups, and ceramide synthase 2 (*Cers2*) favors the transfer of very long-chain (such as C22 and C24) acyl groups.

To identify which isoforms contribute to the induction of ceramide synthesis by WEC treatment, the levels of mRNA encoding those ceramide synthases were analyzed by RT-qPCR. As shown in Fig. 3, we observed no change to *Cers5* mRNA levels upon WEC treatment for any incubation period

(1, 6, or 24 hr). On the other hand, the level of *Cers2* mRNA was significantly increased in WEC-treated cells after 24 hr of incubation. The level of *Cers6* mRNA was slightly higher in WEC cells than in mock-treated cells, although the increase was not statistically significant. Taken together, these observations suggest that induction of the expression of ceramide synthase 2, and possibly ceramide synthase 6 contribute to the increase in the amount of cellular ceramide after WEC treatment.

The level of *Cers2* mRNA was not increased within 6 hr after treatment of WEC. On the other hand, the decreasing of connexin 43 and the depolymerization of actin were observed within 6 hr after WEC treatment both *in vivo* and *in vitro* experiments (Hama et al., 2014). Although the detail mechanism for gene expression of *CerS2* has not been reported (Kim et al., 2021; Levy and Futerman, 2010), we think there would be a possibility that ceramide synthase 2 is induced by rearrangement of intercellular junctions.

4. Conclusion

WEC treatment induces the expression of ceramide synthases, especially ceramide synthase 2. This induction increases the amount of cellular ceramides containing very long-chain acyl groups, such as C22 and C24. We hypothesize that ceramide molecules having such *N*-acyl groups change the property of lipid bilayer and increased ceramide level enhances the permeability of the endosomal membrane, facilitating the release of macromolecules from endosomes into cytoplasm. B16-F1 cell used in this study is derived from mouse skin cell. Therefore, we consider that the results obtained by using intact mouse skin will be similar with that obtained by using B16-F1 cell. Based on the results obtained by *in vitro* experiments, further *in vivo* analyses will be necessary for resolving the mechanism of WEC.

Acknowledgements

We thank Dr. Katsuya Morito (Kyoto Pharmaceutical University, Japan) for technical advice. This work was supported in part by a Tokushima University research program for the development of an intelligent Tokushima artificial exosome (iTEX).

Conflicts of interest

The authors declare that they have no known competing interests.

References

Artetxe I, Ugarte-Uribe B, Gil D, Valle M, Alonso A, García-Sáez AJ, et al. Does Ceramide Form Channels? The Ceramide-Induced Membrane Permeabilization Mechanism. Biophys J 2017; 113: 860-868.

Becker I, Wang-Eckhardt L, Yaghootfam A, Gieselmann V and Eckhardt M. Differential expression of (dihydro)ceramide synthases in mouse brain: oligodendrocyte-specific expression of CerS2/Lass2. Histochem Cell Biol 2008; 129: 233-241.

Bligh EG and Dyer WJ. A rapid method of total lipid extraction and purification. Can J Biochem Physiol 1959; 37: 911-917.

Hama S, Kimura Y, Mikami A, Shiota K, Toyoda M, Tamura A, et al. Electric stimulus opens intercellular spaces in skin. J Biol Chem 2014; 289: 2450-2456.

Hasan M, Nishimoto A, Ohgita T, Hama S, Kashida H, Asanuma H, et al. Faint electric treatment-induced rapid and efficient delivery of extraneous hydrophilic molecules into the cytoplasm. J Control Release 2016a; 228: 20-25.

Hasan M, Tarashima N, Fujikawa K, Ohgita T, Hama S, Tanaka T, et al. The novel functional nucleic acid iRed effectively regulates target genes following cytoplasmic delivery by faint electric treatment. Sci Technol Adv Mater 2016b; 17: 554-562.

Hoeferlin LA, Fekry B, Ogretmen B, Krupenko SA and Krupenko NI. Folate stress induces apoptosis via p53-dependent de novo ceramide synthesis and up-regulation of ceramide synthase 6. J Biol Chem 2013; 288: 12880-12890.

Kajimoto K, Yamamoto M, Watanabe M, Kigasawa K, Kanamura K, Harashima H, et al. Noninvasive and persistent transfollicular drug delivery system using a combination of liposomes and iontophoresis. Int J Pharm 2011; 403: 57–65.

Kalia YN, Naik A, Garrison J and Guy RH. Iontophoretic drug delivery. Adv Drug Deliv Rev 2004; 56: 619–658.

Karpiński TM. Selected Medicines Used in Iontophoresis. Pharmaceutics 2018; 10: 204.

Kigasawa K, Kajimoto K, Nakamura T, Hama S, Kanamura K, Harashima H, et al. Noninvasive and efficient transdermal delivery of CpG-oligodeoxynucleotide for cancer immunotherapy. J Control Release 2011; 150: 256-265.

Kigasawa K, Kajimoto K, Hama S, Saito A, Kanamura K and Kogure K. Noninvasive delivery of siRNA into the epidermis by iontophoresis using an atopic dermatitis-like model rat. Int J Pharm 2010; 383: 157-160.

Kim JL, Mestre B, Shin SH and Futerman AH. Ceramide synthases: Reflections on the impact of Dr. Lina M. Obeid. Cell Signal 2021; 82: 109958.

Leong DJ, Gu XI, Li Y, Lee JY, Laudier DM, Majeska RJ, et al. Matrix metalloproteinase-3 in articular cartilage is upregulated by joint immobilization and suppressed by passive joint motion. Matrix Biol 2010; 29: 420-426.

Levy M and Futerman AH. Mammalian ceramide synthases. IUBMB Life 2010; 62: 347-356.

Perera MN, Ganesan V, Siskind LJ, Szulc ZM, Bielawska A, Bittman R, et al. Ceramide channel: Structural basis for selective membrane targeting. Chem Phys Lipids 2016; 194: 110-116.

Siskind LJ, Kolesnick RN and Colombini M. Ceramide channels increase the permeability of the mitochondrial outer membrane to small proteins. J Biol Chem 2002; 277: 26796-26803.

Taniguchi M and Okazaki T. Role of ceramide/sphingomyelin (SM) balance regulated through "SM cycle" in cancer. Cell Signal 2021; 87: 110119.

Torao T, Mimura M, Oshima Y, Fujikawa K, Hasan M, Shimokawa T, et al. Characteristics of unique endocytosis induced by weak current for cytoplasmic drug delivery. Int J Pharm 2020; 576: 119010.